Master's Degree Thesis
ISRN: BTH-AMT-EX--2006/D-03--SE

Damage Assessment in Thin Materials: Finite Element Investigation

Mirza Mohammed Yousuf Baig

Department of Mechanical Engineering
Blekinge Institute of Technology
Karlskrona, Sweden

2006

Supervisor: Etienne Mfoumou, M.Sc. Mech. Eng.

Damage Assessment in Thin Materials: Finite Element Investigation.

Mirza Mohammed Yousuf Baig

Department of Mechanical Engineering

Blekinge Institute of Technology

Karlskrona, Sweden

2006

Thesis submitted for completion of Master of Science in Mechanical Engineering with emphasis on Structural Mechanics at the Department of Mechanical Engineering, Blekinge Institute of Technology, Karlskrona, Sweden.

Abstract:

This thesis describes the process of detection, and if possible, also localization of the damage in non structural sheet-like materials. Simulation and analysis is carried out in ABAQUS with a FE model that has the same dynamic characteristics as the corresponding real material. Three types of damage forms are investigated: crack, hole and local weakness. Results presented in the report show that global damage detection and localization in sheet-like structure by monitoring changes in the modal parameters is possible. Based on the results, this thesis provides a basis for development of global non-destructive health monitoring methods for materials having no bending stiffness.

Keywords: NDT, Finite Element, ABAQUS, Damage Assessment, Eigenvalue, Stiffness.

.

Acknowledgements

This work was carried out at the Department of Mechanical Engineering, Blekinge Institute of Technology, Karlskrona, Sweden, under the supervision of M.Sc. Etienne Mfoumou.

I wish to express my sincere appreciation to M.Sc Etienne Mfoumou for his guidance and professional engagement throughout the work.

I wish to express my sincere appreciation to my mother Mrs Khursheed Kausar and my father Mr Mirza Masood Hassan for their invaluable assistance and encouragement during this Masters Education.

Karlskrona, January 2006

Mirza Mohammed Yousuf Baig

Contents

1 Notation

A	*Amplitude[m]*
a	*Width[m]*
b	*Length[m]*
c	*Velocity[m/s]*
D	*Stress-strain constitutive matrix [-]*
F	*Global force matrix [-]*
f	*Frequency[Hz]*
G	*Energy release rate [J/s]*
h	*Thickness of material[m]*
J	*Jacobian matrix [-]*
K	*Global stiffness matrix*
K^{MN}	*Stiffness matrix [-]*
k	*Nodal stiffness matrix[-]*
L	*Length[m]*
M^{MN}	*Mass matrix [-]*
N_c	*Number of elements [-]*
N_i	*Shape functions [-]*
T	*Tensile Force [N]*
t	*Time[s]*
$[u]$	*Displacement matrix [-]*
u	*Displament in an elment in x-direction[m]*
u_i	*Nodal displacement[m]*
v	*Displacement in an element in y-direction[m]*
v_i	*Nodal displacement[m]*
W	*Length[m]*

w	*Angular velocity [rad/sec]*
ω	*Strain energy density [J/m^3]*
ε	*Displacement[m]*
ρ	*Density of material [Kg/m^3]*
$\{\varepsilon\}$	*Strain matrix at (x, y) [-]*
σ	*Stress matrix [-]*
$\prod$	*Potential energy [J]*
Γ_0	*Set of elements [-]*
Γ_1	*Set of elements [-]*
ϕ^N	*Eigenvector [-]*

Indices

I	*Node*
j	*Node*
load	*Fixed load conditions*
M	*Degree of freedom*
N	*Degree of freedom*
n	*Number of nodes in the element*
nm	*Mode numbers*

Abbreviations

FEM	Finite Element Method
BTH	Blekinge Tekniska Hogskola
NDT	Non Destructive Testing
ELSE	Total elastic strain energy in the element

2 Introduction

The ability to monitor a structure and detect damage before it reaches critical levels is of outmost importance in sheet-like materials used in food packages. Additional global damage detection techniques are of interest and this has led to development of methods that examine changes in the dynamic characteristics of structures. The concept behind these methods is that damage in a structure changes the modal parameters because they are functions of the mechanical and physical properties of the structure.

This work will first focus on level I damage identification on sheet-like material, as classified by *Doebling [1]*. Following defects will be investigated:

- Local weakness
- Hole
- Crack

The aim of the work is to develop a simulation model corresponding to the material under study, which will predict the material behaviour after introduction of a scatter in form of defects listed above. The results may serve as indicator for realisation of an appropriate experimental setup.

Simulation is an important tool when it comes to visualize results which might be difficult or in many cases impossible to achieve experimentally. In case of material with high contact sensitivity, the simulation model is thus of vital importance to visualize such results and use the results to develop a non destructive testing measurement technique, optimize or correct an existing one. The results from experimental studies have been used during this study. This kind of co-operation between simulation and experimental results forms the basis of the approach used, permitting validation of the implemented model.

Chapter 3 starts with an overview of the three types of defects investigated during the study. A reference is given to another work which deals in detail with the techniques of detection at the end of the chapter.

Chapter 4 presents a mathematical model for the thin vibrating membrane.

Chapter 5 gives an overview of the experimental setup for which the subsequent experimental results were obtained.

Chapter 6 gives a background of the numerical analysis and approaches used during the study.

Chapter 7 presents modelling details for the defects.

Chapter 8 presents the results and interpretation of the results for the types of defects.

Chapter 9 gives conclusion and further work from this work.

3 Overview of Defects

3.1 Types of Defects

Defects and damages cause the thin laminates to lose their strength and rigidity and also the safe working life is reduced. Defects and damages can creep in at any time like manufacturing, in service or in design due to discontinuities such as cut out and play drops. The defects and damages under investigation in this study are presented in figure 3.1 below.

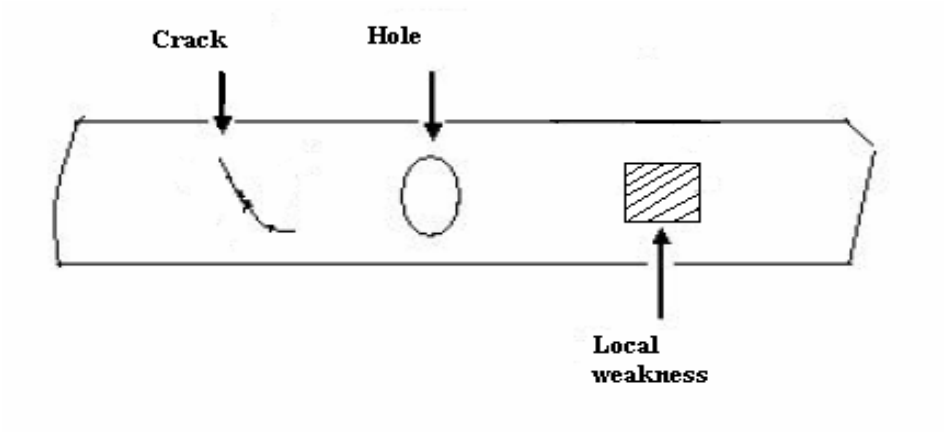

Figure 3.1 illustrating the three kinds of defects.

3.1.1 Local Weakness

A local weakness is a type of defect in which the material losses its stiffness in some proportion to the original stiffness. The defect intensity increases with increased proportionality. It is caused by the rubbing of the surfaces.

3.1.2 Hole

A hole is an opening through the material. It can be of any shape, although for simplicity we consider it to be a circle.

3.1.3 Crack

Cracks are one of the most common types of defects .A crack is a long narrow opening through the material. We consider the crack to have sharp tips.

Some conventional and non conventional methods commonly employed in the industries to experimentally detect these defects were presented in [2].

4 Theoretical Analysis

The theoretical model is based on assumptions made regarding the geometry, material conditions, loading, and displacement boundary conditions.

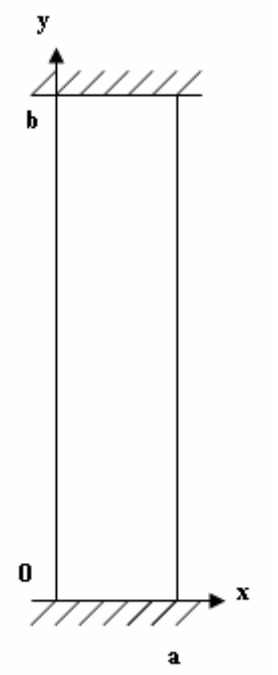

Figure 4.1 illustrating the specimen clamped along the width and free along the height.

Let us denote:

T: Tensile force per unit length along the width
ε : Displacement of a given point (x, y) in the z-direction
ρ : Density of material
h: Thickness of the material

The differential equation describing vibration is:

$$\frac{\partial^2 \varepsilon}{\partial t^2} = \frac{T}{\rho h}\left(\frac{\partial^2 \varepsilon}{\partial x^2} + \frac{\partial^2 \varepsilon}{\partial y^2}\right) \qquad (4.1)$$

Let us denote $\frac{T}{\rho h} = c^2$, where c is the velocity of wave propagation.
It follows that the velocity c can be monitored by variation of the applied force.

The Boundary conditions are defined as follows,

x = 0, x = a are free
y = 0, y = b are fixed

The solution of equation (4.1) is in the following form:

$$\varepsilon = A\cos\left(\pi m \frac{x}{a}\right)\sin\left(\pi n \frac{y}{b}\right)\cos wt \qquad (4.2)$$

Inserting (4.2) into (4.1) and solving for natural frequencies leads to the following expression:

$$\omega_{mn} = c\sqrt{\left(\frac{\pi m}{a}\right)^2 + \left(\frac{\pi n}{b}\right)^2} \qquad (4.3)$$

$$\omega_{mn} = 2\pi f_{mn} \Rightarrow f_{mn} = \frac{c}{2\pi}\sqrt{\left(\frac{\pi m}{a}\right)^2 + \left(\frac{\pi n}{b}\right)^2} \qquad (4.4)$$

5 Available experimental results

5.1 Experimental procedure

The component under study may be mechanically characterized by the response of the component by the mechanical excitation. Such an excitation can be achieved externally by a pulsed or periodical loading.

The case study under investigation is a single layered material (paperboard) clamped on both the upper and lower edges merging them into edges. The tensile test machine is used for the loading. As a thin layer possesses no compression or bending stiffness it is required to pre-stress the structure in order to make it act like a structural element. Hence the specimen is loaded within its elastic region just to produce bending wave's propagation from a periodic acoustic load.

The specimen has a surface tension of 20 mN/m and a mean thickness of h = 0.1 mm. The length is L = 0.65 m and the width is W = 0.012 mm. The acoustic load is provided by a loudspeaker having 4-8 ohm impedance, and a broad frequency range of 70 to 20.000 Hz, located around the middle of the specimen. Using an Agilent function generator the excitation frequency can be tuned continuously. A picture of the experimental setup is shown in figure 5.1.

A basic understanding of the experimental setup for the natural frequency extraction is necessary. The results obtained from this experiment are used as inputs to the simulation model and for the correlation with the simulation results. This will also lead to the validation of the FEM model created.

The specimen was excited using a 10 V sine sweep signal, which was sent to the loudspeaker through a function generator to drive it between 0 and 900 Hz for the control specimen as well as for each damage case. The middle of the specimen was chosen as region of excitation, leading to strong excitation of odd modes of vibration. The method is to monitor the amplitude of the signal received in the time domain by a VS-100 OMETRON laser vibrometer, using A scans at the middle of the material. The laser signal fed to a high-pass/low-pass filter assures that only the excited frequency range is included in the velocity reading.

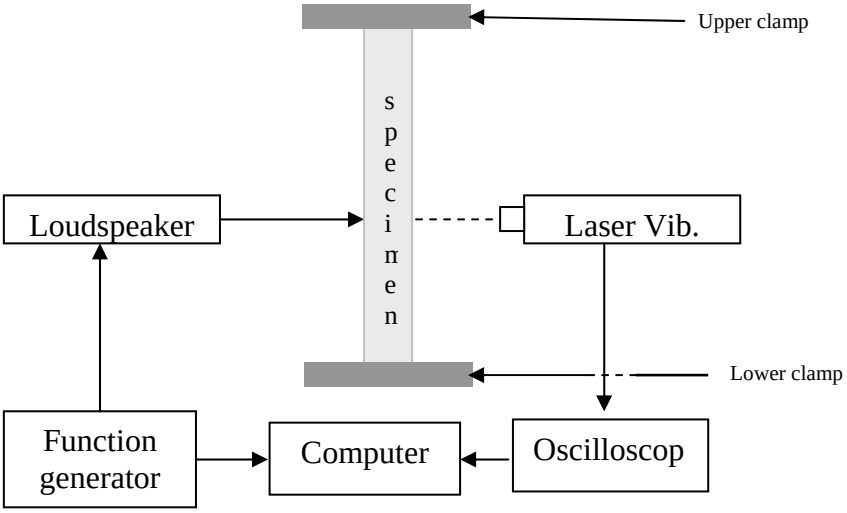

Figure 5.1 illustrates the experimental setup.

5.2 Results

Following are the results obtained from the above experimental setup. These results have been used as inputs to the simulation model in ABAQUS.

Table 5.1 available experimental result.

Fundamental Frequency Hz	107.9 Hz
Young's Modulus Mpa	8e9 MPa

6 Overview of Numerical Analysis

In Limited cases it is possible to obtain a closed form analytical solution for natural frequency extraction in a structure that is subjected to a static loading with a defect induced. A variety of numerical techniques have been applied to problems in numerical analysis including finite difference, finite element and boundary integral equation methods. In recent years the latter two numerical methods have been applied almost exclusively. The vast majority of defected structures use finite elements, although the boundary integral method may be useful in limited circumstances.

6.1 The finite element method

The structure of interests is subdivided into discrete shapes called elements. The most common element types include one-dimensional beams, two dimensional plain stress or plain strain elements and three dimensional bricks or tetrahedrons. The elements are connected at node points where continuity of displacements fields is enforced.

Figure 6.1 shows an isoparametric continuum element for two dimensional plane stress or plane strain problems together with local and global co-ordinate axes. The Local co-ordinates which are called parametric co-ordinates vary from -1 to +1 over the element area; the nodes at the lower left hand corner has parametric co-ordinates (-1,-1). While upper hand corner is at (+1, +1) in the local system. Note that the parametric coordinate system is not necessarily orthogonal. Consider a point on the element at (ξ,η). The global coordinates of this point are given by,

$$x = \sum_{i=1}^{n} N_i(\xi,\eta)x_i \qquad (6.1)$$

$$y = \sum_{i=1}^{n} N_i(\xi,\eta)y_i \qquad (6.2)$$

Where n is the number of nodes in the element and N_i are the shape functions corresponding to the node i, whose coordinates are (x_i, y_i) in the global system and (ξ_i, η_i) in the parametric system.

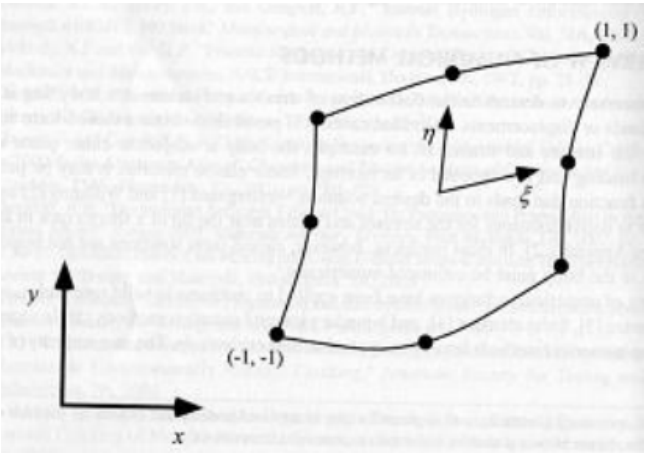

Figure 6.1 illustrates an isoparametric continuum element.

The shape functions are polynomials that interpolate field quantities within the element. The degree of the polynomial depends on the number of nodes in the element. If for example the elements contain the nodes only at corners, N_i are linear. Figure above illustrates a four sided eight node element which requires a quadratic interpolation.

The displacements within each element are interpolated as follows:

$$u = \sum_{i=1}^{n} N_i(\xi, \eta) u_i \qquad (6.3)$$

$$v = \sum_{i=1}^{n} N_i(\xi, \eta) v_i \qquad (6.4)$$

Where (u_i, v_i) are the nodal displacements in the x and y directions, respectively. The strain matrix at (x, y) is given by,

$$\begin{Bmatrix} \varepsilon_x \\ \varepsilon_y \\ \gamma_{xy} \end{Bmatrix} = [B] \begin{Bmatrix} u_i \\ v_i \end{Bmatrix} \tag{6.5}$$

$$[B] = \begin{bmatrix} \frac{\partial N_i}{\partial x} & 0 \\ 0 & \frac{\partial N_i}{\partial y} \\ \frac{\partial N_i}{\partial y} & \frac{\partial N_i}{\partial x} \end{bmatrix} \tag{6.6}$$

$$\begin{Bmatrix} \frac{\partial N_i}{\partial x} \\ \frac{\partial N_i}{\partial y} \end{Bmatrix} = [J]^{-1} \begin{Bmatrix} \frac{\partial N_i}{\partial \xi} \\ \frac{\partial N_i}{\partial N} \end{Bmatrix} \tag{6.7}$$

Where $[J]$ is the Jacobian matrix which is given by,

$$[J] = \begin{bmatrix} \frac{\partial x}{\partial \xi} & \frac{\partial y}{\partial \xi} \\ \frac{\partial x}{\partial \eta} & \frac{\partial y}{\partial \eta} \end{bmatrix} = \begin{bmatrix} \frac{\ldots \partial N_i \ldots}{\partial x} \\ \frac{\ldots \partial N_i \ldots}{\partial y} \end{bmatrix} \begin{bmatrix} .. \\ x_i y_i \\ .. \end{bmatrix} \tag{6.8}$$

The stress matrix is computed as follows:

$$\{\sigma\} = [D]\{\varepsilon\} \tag{6.9}$$

Where [D] is the stress-strain constitutive matrix. For problems that incorporate incremental plasticity stress and strain are computed incrementally and [D] is updated at each step:some p

$$\{\Delta\sigma\} = [D(\varepsilon,\sigma)]\{\Delta\varepsilon\} \qquad (6.10)$$

Thus the stress and strain distribution throughout the body can be inferred from the nodal displacements and constitutive law. The stresses and strains are usually at several gauss points or integration points within each element. For two dimensional elements 2×2 Gauss integration is typical where there are four integration points on each element.

The displacements at the nodes depend on the element stiffness and nodal forces. The nodal stiffness matrix is given by,

$$[k] = \int_{-1}^{1}\int_{-1}^{1} [B]^T [D][B]\det|J|d\xi d\eta \qquad (6.11)$$

Where the superscript *T* denotes the transpose of the matrix. Equation above can be derived from the principal of minimum potential energy.

The elemental stiffness matrices are assembled to give the global stiffness matrix $[\mathrm{K}]$. The global force, displacement and stiffness matrices are related as follows:

$$[\mathrm{K}][u] = [F] \qquad (6.12)$$

6.2 Methods for the crack analysis

Several references of the earlier approaches for inferring crack analysis parameters from numerical analysis exist in literature [3] [11, 12, 15, 16 see page 590]. Most of these methods have been made obsolete by more recent techniques that are significantly more accurate and efficient. The virtual crack extension approach, used in ABAQUS, is presented below.

6.2.1 Virtual crack extension: Stiffness derivative formulation

This method was proposed by Parks and Hellen [4, 5] for inferring energy release rate in elastic bodies. Although the stiffness derivative method is now outdated it was a precursor to the modern approach, the widespread energy domain integral [6, 7],

For illustration, consider a two-dimensional body with unit thickness, subject to Mode 1 loading. The potential energy of the body in terms of finite element solution is given by,

$$\Pi = \frac{1}{2}[u]^T [K][u] - [u]^T [F] \qquad (6.13)$$

Where Π is the potential energy and other quantities as previously defined. The energy release rate is the derivative of Π with respect to crack area, for both fixed load and fixed displacement conditions. It is convenient under in this instance to evaluate G under fixed load conditions.

$$G = -\left(\frac{\partial \Pi}{\partial a}\right)_{load}$$
$$= -\frac{\partial [u^T]}{\partial a}\{[K][u] - [F]\} - \frac{1}{2}[u]^T \frac{\partial [K]}{\partial a}[u] + [u^T]\frac{\partial [F]}{\partial a} \qquad (6.14)$$

Comparing equation (6.12) to the above result, we see that the first term in equation (6.13) must be zero. In the absence of tractions on the crack faces, the third term must also vanish, since loads are held constant. Thus the energy release rate is given by,

$$G = \frac{K_I^2}{E'} = -\frac{1}{2}[u]^T \frac{\partial [K]}{\partial a}[u] \qquad (6.15)$$

It follows from the above equation that the energy release rate is proportional to the derivative of stiffness matrix with respect to crack length.

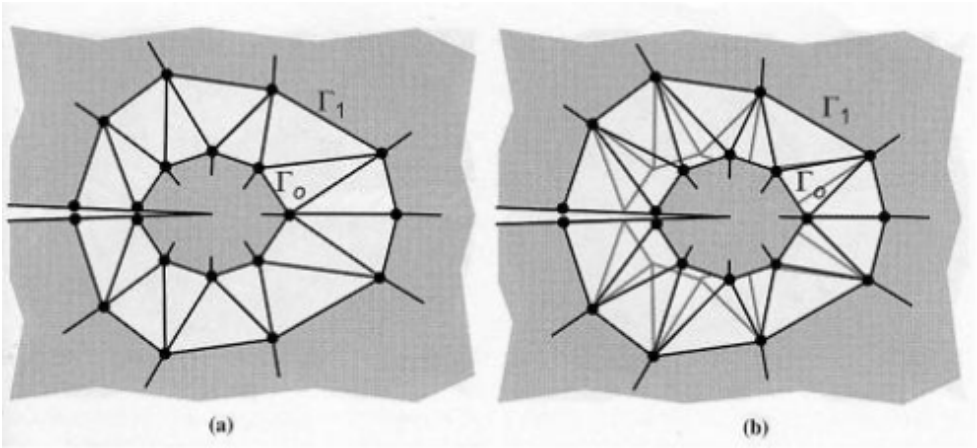

Figure 6.2 illustrates crack extension from (a) to (b) and the two countours around the crack tip.

However, if a finite element mesh is generated for a body with crack length a and we wish to extend the crack by Δa in order to simulate a more severe defect behaviour, it would not be necessary to change all of the elements in the mesh; we would accommodate the elements by changing the crack growth by moving the elements near the crack tip and leaving the rest of the mesh intact. Above figure illustrates such a process where elements inside the contour Γ_0 are shifted by Δa, and elements outside the contour Γ_1 are unaffected. Each of the elements between Γ_0 and Γ_1 is distorted, such that its stiffness changes. The energy release rate is related to this change in element stiffness:

$$G = -\frac{1}{2}[u]^T \left(\sum_{i=1}^{N_e} \frac{\partial [k_i]}{\partial a} \right) [u] \qquad (6.16)$$

Where $[k_i]$ are the elemental stiffness matrices and N_c is the number of elements between the contours Γ_0 and Γ_1. It is important to note that in this approach, it is not necessary to generate a second mesh with slightly longer crack. It is sufficient merely to calculate the change in elemental stiffness matrices corresponding to shifts in the nodal coordinates.

6.2.2 Virtual Crack Extension: Continuum Approach

Parks and Hellen formulated the virtual crack extension approach in terms of finite element stiffness and displacement matrices. This was improved by considering the energy release rate of a continuum. The main advantages of the continuum approach are twofold: first, the methodology is not restricted to the finite element method; and second the method does not require numerical differencing.

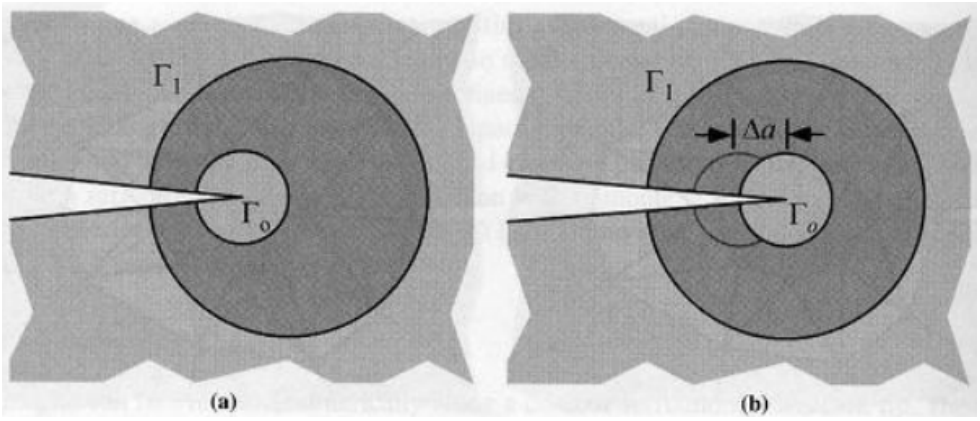

Figure 6.2 illustrates virtual crack advance from (a) to (b) in a two dimensional continuum.

Figure (6.2) illustrates a virtual crack advance in a two-dimensional continuum. Material points inside Γ_0 experience rigid body translation of a distance Δa in the x_1 direction, while points outside of Γ_1 remain fixed. In the region between contours, virtual crack extension causes material points

to translate by Δx_i. For an elastic material, or one that obeys deformation plasticity theory, it was shown that energy release rate is given by,

$$G = \frac{1}{\Delta a}\int_A \left(\sigma_{ij} \frac{\partial u_j}{\partial x_1} - w\delta_{i1} \right) \frac{\partial \Delta x_1}{\partial x_i} dA \qquad (6.17)$$

where ω is the strain energy density. Equation above assumes unit thickness, crack growth in the x_1 direction, no body forces within Γ_1, and no tractions on the crack faces. Note that $\partial \Delta x_1 / \partial x_i = 0$ outside of Γ_1 and within Γ_0; thus the integration need only be performed over the annular region between Γ_0 and Γ_1.

7 Simulation

7.1 Problem formulation

For the finite-element analysis, we use the commercially available software ABAQUS. A rectangular membrane with a symmetric, centrally located scatter is subject to natural frequency extraction. Scatterer is defined as semi-elliptic part-through crack, hole and local weakness. The objective is to estimate modal parameter changes due to scatter for use as damage indicator. Focus is put on levels I and II damage assessment. Eigenvalue extraction is used for the analysis.

7.1.1 Eigenvalue technique

The frequency extraction procedure uses eigenvalue techniques to extract the frequencies of the current system. The eigenvalue problem for the natural frequencies of an undamped finite element model is,

$$\left(-\omega^2 M^{MN} + K^{MN}\right)\phi^N = 0 \qquad (7.1)$$

where,

M^{MN} is the mass matrix (which is symmetric and positive definite);

K^{MN} is the stiffness matrix (which includes initial stiffness effects if the base state included the effects of nonlinear geometry);

ϕ^N is the eigenvector (the mode of vibration);

and *M* and *N* are degrees of freedom.

If initial stress effects are not included and there are no rigid body modes, K^{MN} is positive definite; otherwise, it may not be. Negative eigenvalues normally indicate instability.

7.1.2 Definition of the models

Linear elastic behavior and membrane elements are used to model the material. Membrane elements are often used to represent thin surfaces in space that offer strength in the plane of the element but have no bending stiffness.

On the other hand, we are dealing with a thin membrane. Therefore the transverse shear and rotary inertia are neglected and an isotropic material behavior is assumed. In this case, only Young's modulus and Poisson's ratio are needed.

An eigenvalue analysis is performed with a *FREQUENCY* step, for natural frequency extraction using the Lanczos eigensolver. No load and no interaction are applied to the material, which reduces the problem to the investigation of the modes of the unloaded material.

7.1.3 Elements

The element type M3D4R is used to model the material. It is a three-dimensional four-node membrane element with reduced integration. Reduced integration provides accurate results at a significantly less running time. Membrane elements are sheets in space that can carry membrane force but do not have any bending or transverse shear stiffness, so the only nonzero stress components in the membrane are those components parallel to the middle surface of the membrane, therefore the membrane is in a state of plane stress.

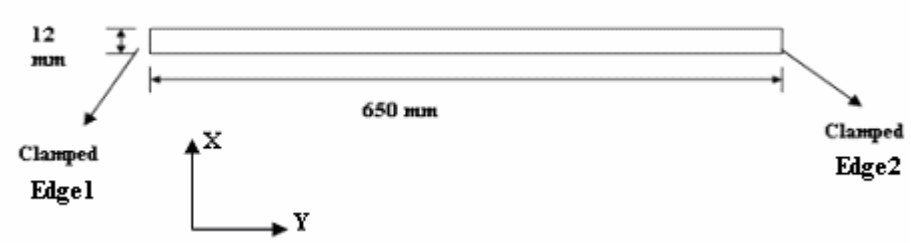

Figure 7.1 illustrates the control specimen’s geometry and boundary conditions.

7.1.4 Convergence study

Mesh resolution is an important factor; models have been tested with multiple mesh resolutions. Some factor that the mesh resolution influences are computational time and accuracy of the results [8]. Following are the results from Abaqus for convergence test conducted to decide the best mesh size.

The specimen was divided into three partitions as shown in figure 7.2 in order to refine the mesh surrounding the area. The defect was placed in the second partition, P_2. Element size with an area 0.000882 m^2 was found to be appropriate for the partitioned area P_1 and $P_{1,}$ while an element with an area 0.00001 m^2 was appropriate for area P_2.

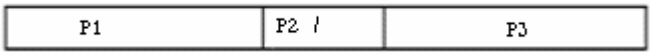

Figure 7.2 illustrates the specimen divided into three partitions.

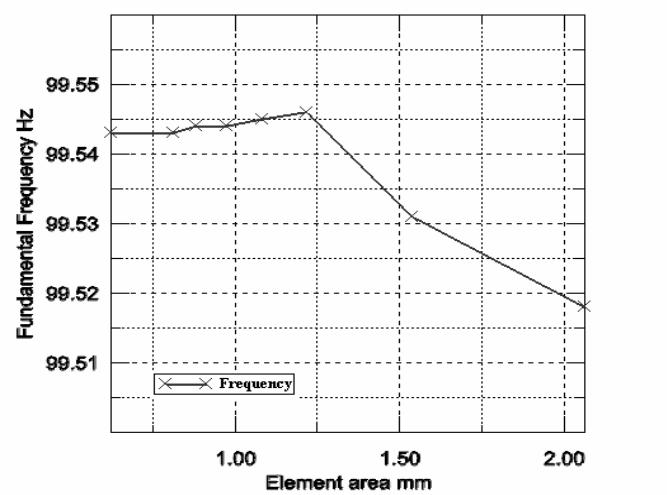

Figure 7.3 shows the frequency converging after a certain element size is reached; the above mesh size is for the area P_1 and P_3.

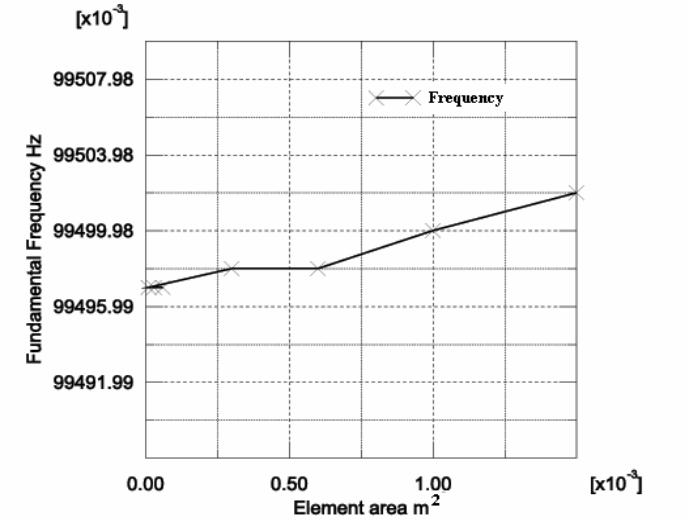

Figure 7.4 shows the frequency converging after a certain element size is reached; the above mesh size is for the area P_2.

7.1.5 Boundary conditions

The specimen is clamped on both the ends within the elastic region. There is no movement in any direction.

Table 7.1 Boundary conditions at the Edge 1 as illustrated figure 7.1.

(1)	X	Y	Z
Translation	Fixed-0	Fixed-0	Fixed-0
Rotation	Fixed-0	Fixed-0	Fixed-0

Table 7.2 Boundary conditions at the Edge 2 as illustrated figure 7.1.

(2)	X	Y	Z
Translation	Fixed-0	Fixed-0	Fixed-0
Rotation	Fixed-0	Fixed-0	Fixed-0

7.2 Material details and assumptions

The specimen is a thin single layer membrane 650 mm in length and 12 mm width in geometry and has the following mechanical properties.

Table 7.3 Material Properties.

Density (kg/mm^3)	684
Young's Modulus($N/m^{2)}$	8e9
Poisson's Ratio	0.38
Thickness (m)	0.0001

Assumptions

1. The Material was assumed to be isotropic.
2. Poisson's ratio was assumed to be 0.38.
3. The Material was assumed to be linearly elastic.

7.3 Modeling and Postprocesing

The specimen is clamped at both the edges restricting any movement in any direction. The Thickness, Young's modulus, Poisson's ratio and mass density were given as inputs.

The whole FEM model consists of four sub-models,

I. Control Specimen

II. Model with the introduction of crack

III. Model with introduction of a hole

IV. Model with introduction of a local weakness

The steps for the construction of the model are described in Appendix A. The following sections illustrate the modeling of the defect.

7.3.1 Crack

The crack is modeled as an elliptical removal of mass with the corresponding mesh shown below. Nodal coordinates of elements at the crack tip are changed in order to represent a slightly longer crack.

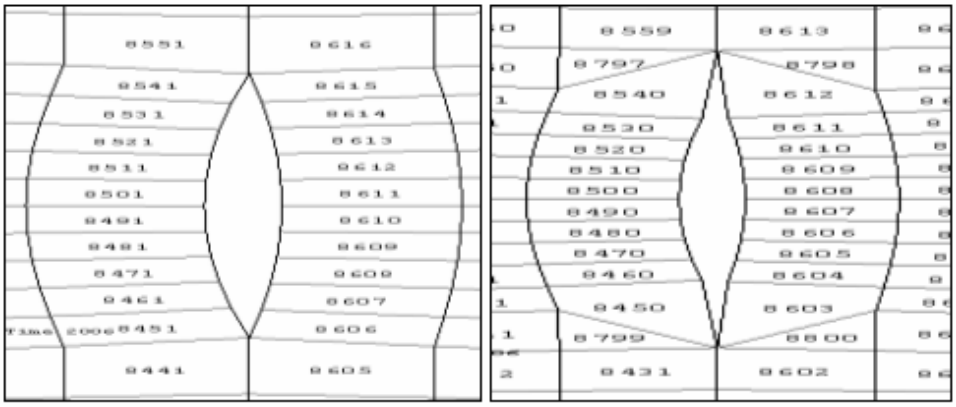

(a) *(b)*

Figures 7.5(a), (b) shows cracks lengths of 4 mm, 5.7 mm respectively. The element labels near to the crack tips can also be seen.

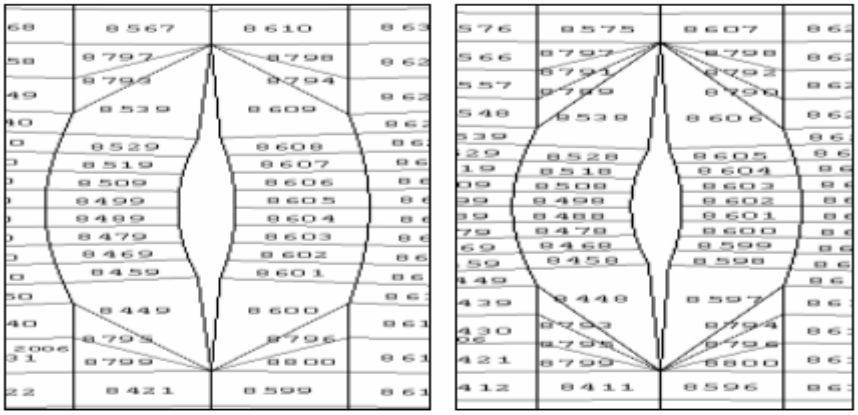

(c) *(d)*

Figures7.6(c), (d) shows cracks lengths of 7.3 mm, 8.8 mm respectively. The element labels near to the crack tips can also be seen.

The correspondences in monitored element labels are as shown below. The correspondences in monitored element labels are as shown below. Crack sizes in figure 7.6 (a), (b), (c) and (d) relate to Model 1, 2, 3 and 4 respectively. Corresponding elements on the other edge are also investigated and give the same result.

Table 7.4 Showing elements investigated and their corresponding labels in different models.

Models	Model 1	Model 2	Model 3	Model 4
Element Label	8616	8798	8794	8790
	8551	8797	8793	8789

As the nodal coordinates at the crack tip are changed, elements connected to the tip will collapse, becoming triangular and leading to change in stiffness, thus in energy as illustrated on equation 6.16 above. The driving

force needed for crack extension being ignored in this study, the singularity at the crack tip is not considered in the developed model.

7.3.2 Hole

The hole is modelled as a circular and noticeable removal of mass in the centre of the geometry. Corresponding meshes are shown below for increasing diameter of the hole.

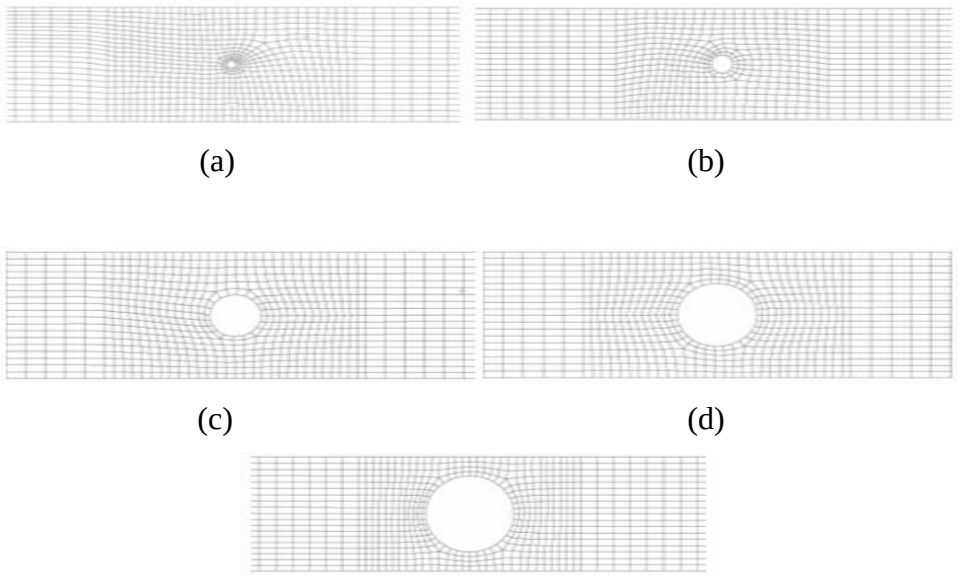

Figure7.7 Shows Holes of different diameter (a) 0.004 m (b) 0.001 m (c) 0.002 (d) 0.003 (e) 0.004.

The hole being just seen as a reduction of the global mass of the structure, no singularity appears around the defect, and no special demand is put on the modelling.

7.3.3 Local weakness

This type of defect is a structural damage which is either brittleness or fragility. The brittleness is the weakness of the material caused by inherent acidity of the material, which can result in its snapping, cracking, or breaking upon handling or folding. The fragility, the type concerned in this study, is the weakness caused by handling, which can lead to immediate tearing.

The local weakness is modelled in two ways,

1. As a change (reduction) in local stiffness of the material, thus, a change in the local rigidity. The locally weak area is changed here and frequency recorded as suggested by table A .5.
2. As a change (reduction) in local stiffness of the material with a constant percentage for the same locally weak area as suggested by tables A.6, A.7 and A.8.

Corresponding meshes are shown on the figures below.

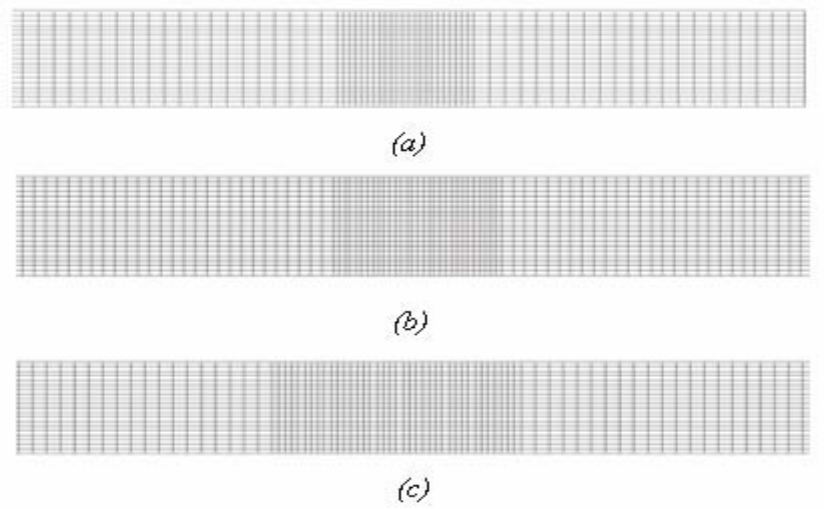

Figure 7.8 shows a local weakness with different areas (a) 0.036 (b) 0.06 (c) 0.072.

8 Results and interpretation

8.1 Crack

The fundamental frequency decreases with an increase in defect severity as seen on figure 8.1 below. This might be connected to the decrease in stiffness (due to scatterer in form of crack) of the element set forming the defect.

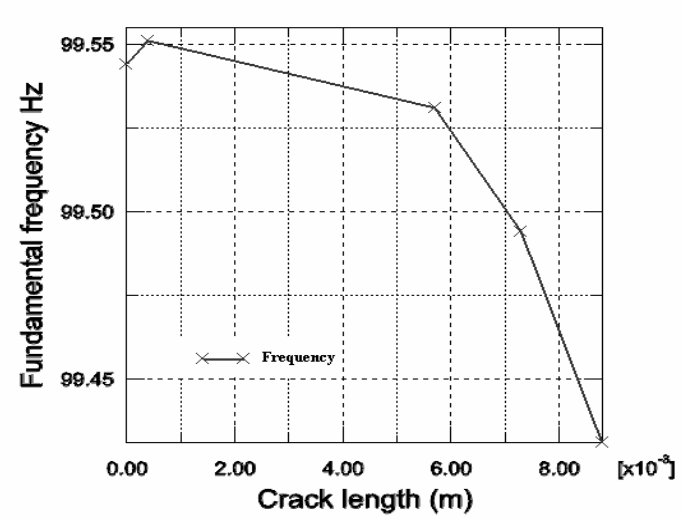

Figure 8.1 relation between the fundamental frequency and the crack length.

It is also observed from the table 8.1 below that, for the fundamental frequency, the elastic strain energy magnitudes (ELSE) of elements connected to the crack tip decrease with an increase in defect severity. Indeed, the strain energy is the amount of potential energy stored in a body by virtue of an elastic deformation, equal to the work that must be done to produce both normal and shear strains**.** Subsequent analyses may focus on higher modes. This strain energy appears to increase at higher modes, with a noticeable peak at mode 12, which corresponds to the mode at which the defect expresses itself as can be observed on figure 8.2 below.

Table 8.1: Strain energy magnitude (ELSE) for an element at the crack tip, for crack lengths 4mm (model 1), 5.7mm (model 2), 7.2mm (model 3), and 8.8mm (model 4).

Mode	ELSE at crack tip			
	Model 1	Model 2	Model 3	Model 4
1	4.6058E-03	3.2776E-03	2.3396E-03	1.9275E-03
2	1.2319E-03	9.8200E-04	1.4867E-03	1.5949E-03
3	0.1982	0.1411	0.1007	8.2864E-02
11	5.489	4.383	6.658	7.173
12	119.5	93.13	47.38	30.76
13	17.45	12.45	8.914	7.258

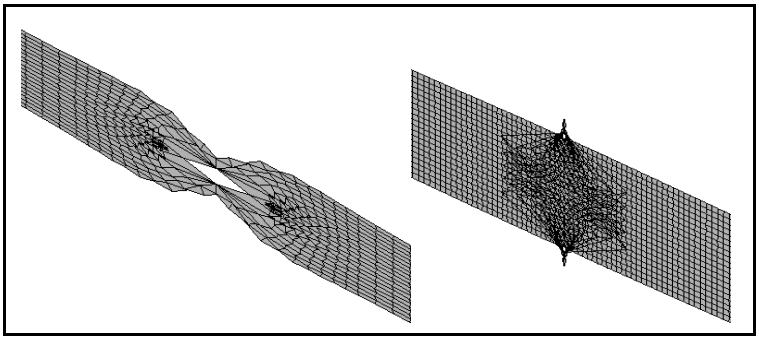

Figure 8.2 Mode 12 illustrating the physical distortion at the defect from the first frame to the last one.

8.2 Hole

The fundamental frequency increases when the diameter of the defect increases as shown on figure 8.3 below.

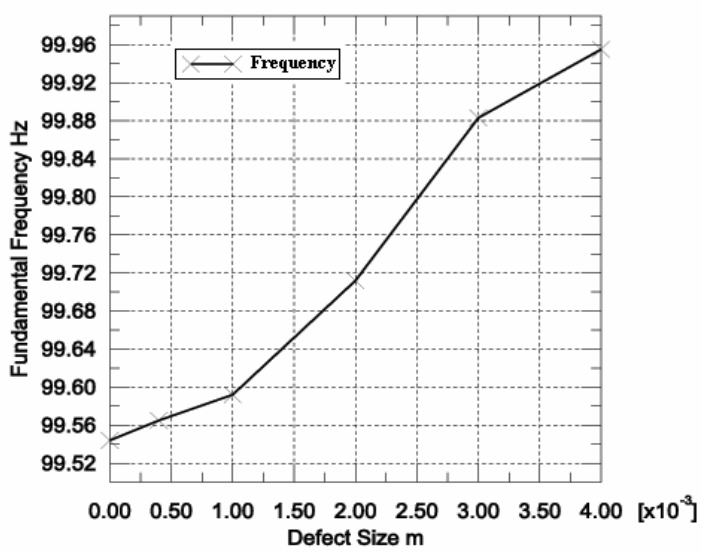

Figure 8.3 relation between the fundamental frequency and the hole diameter.

The observed tendency illustrates a linear behaviour. In fact, for simple vibration of structures, the frequency is inversely proportional to the square root of the mass. Therefore, the frequency increases when the global mass decreases.

As previously, the defect will express itself at mode 12. It may also be shown that the elastic strain energy will peak at this mode for elements affected by the strong distortion as illustrated on figure 8.4 below.

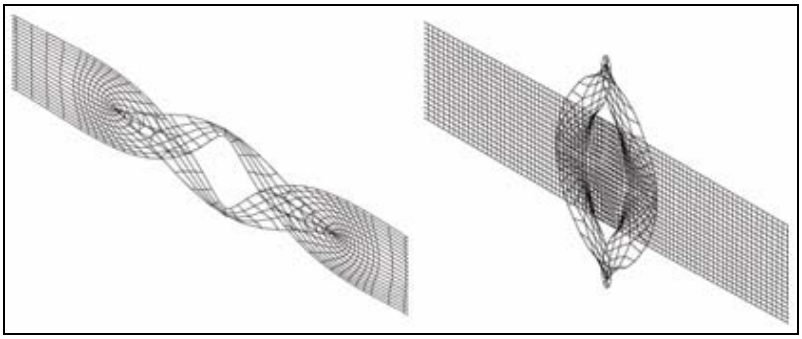

Figure 8.4 Mode 12 illustrating the physical distortion at the defect from the first frame to the last one.

8.3 Local weakness

The results presented in the figure 8.5 shows that the fundamental frequency decreases when the severity of the defect increases.

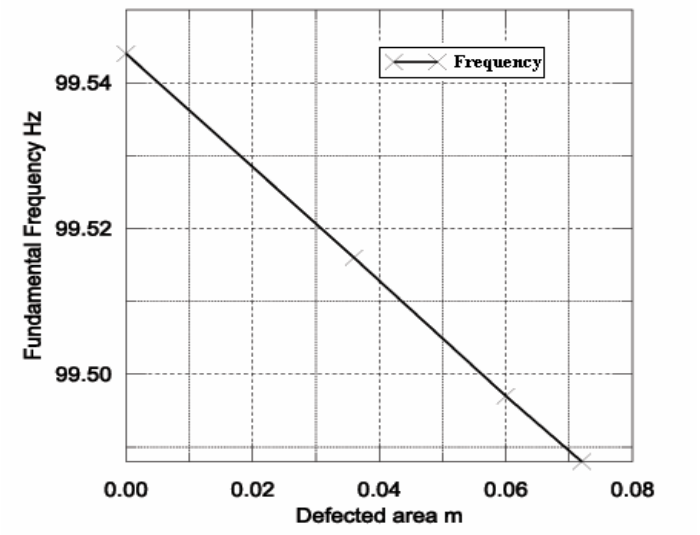

Figure 8.5 relation between the fundamental frequency and the locally weak area.

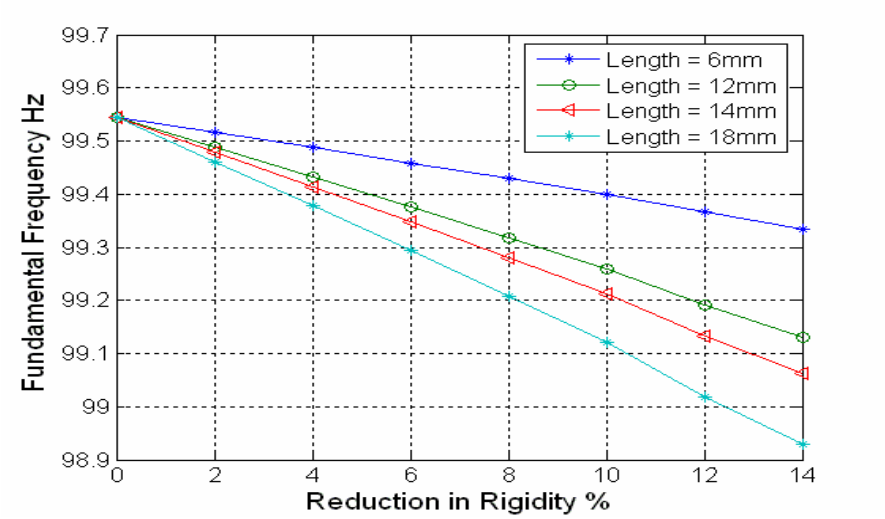

Figure 8.6 relation between the fundamental frequency and a constant change in rigidity for different defect areas.

Results from the first and second approach as described in chapter 7 can be seen in figure 8.5 and 8.6 respectively. From the second approach we can observe that as the defected area increases combined with a constant decrease in the rigidity the curve for the most severe defect tends to have an increase in slope.

As previously, the defect will express itself at mode 12. It may also be shown that the elastic strain energy will peak at this mode for elements affected by the strong distortion as illustrated on figure 8.7.

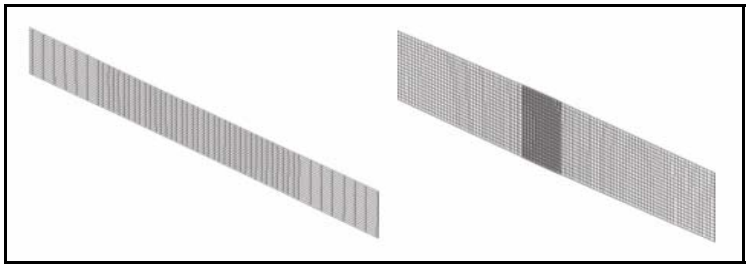

Figure 8.7 Mode 12 illustrating the physical distortion at the defect from the first frame to the last one.

8.4 Spatial distribution of some of the modes

The results shown in this section were obtained from the mathematical model of the undamaged specimen in MATLAB. The aim is to show the ability to detect the defect at higher modes. The following convention is adopted:

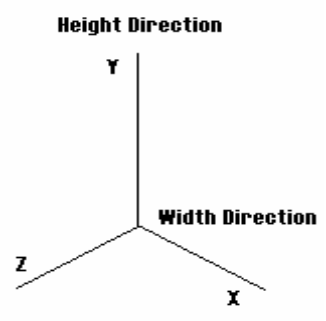

Figure 8.8 convention used for investigating modes in length and width direction.

For better understanding, mode *m_n* denotes the combination of the m^{th} mode in the length direction with the n^{th} mode in the width direction.

Following results were obtained:

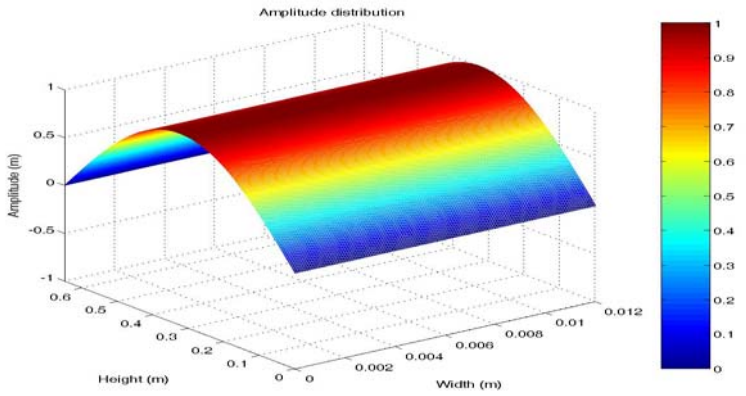

Figure 8.9 Mode 1_0 (100.46Hz).

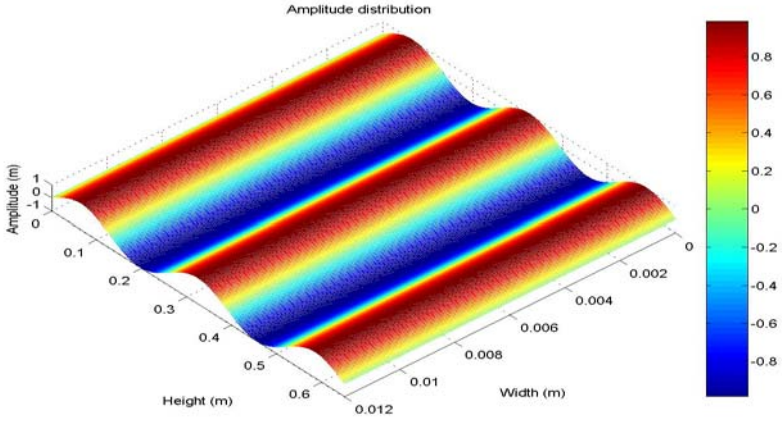

Figure 8.10 Mode 5_0 (500.31Hz).

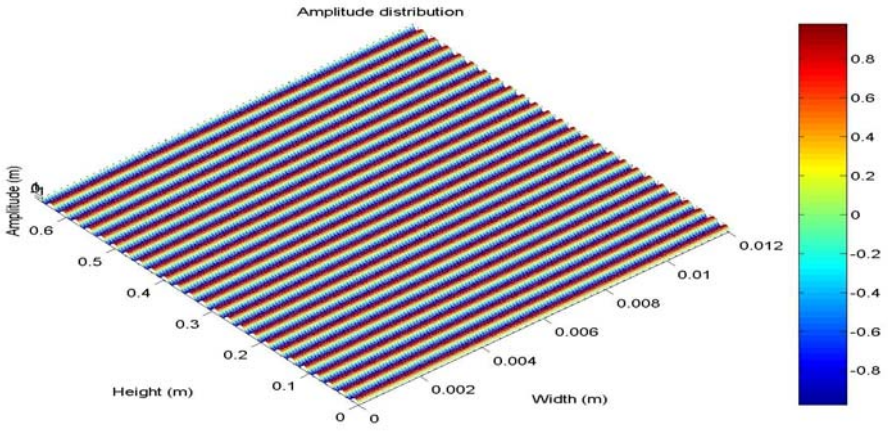

Figure 8.11 Mode 50_0 (5023.1Hz).

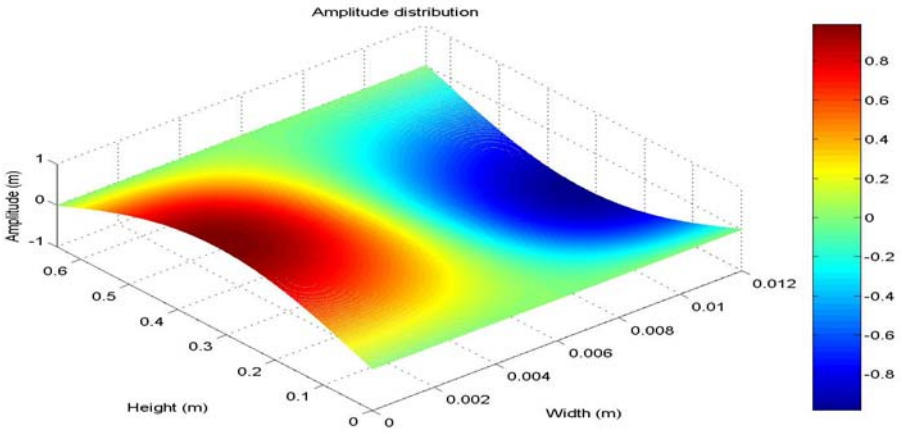

Figure 8.12 Mode 1_1 (5442.6Hz).

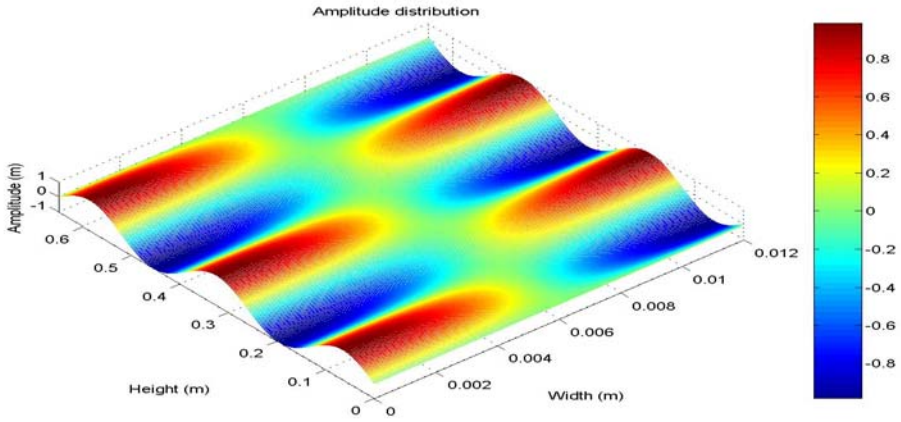

Figure 8.13 Mode 1_5 (5464.8Hz).

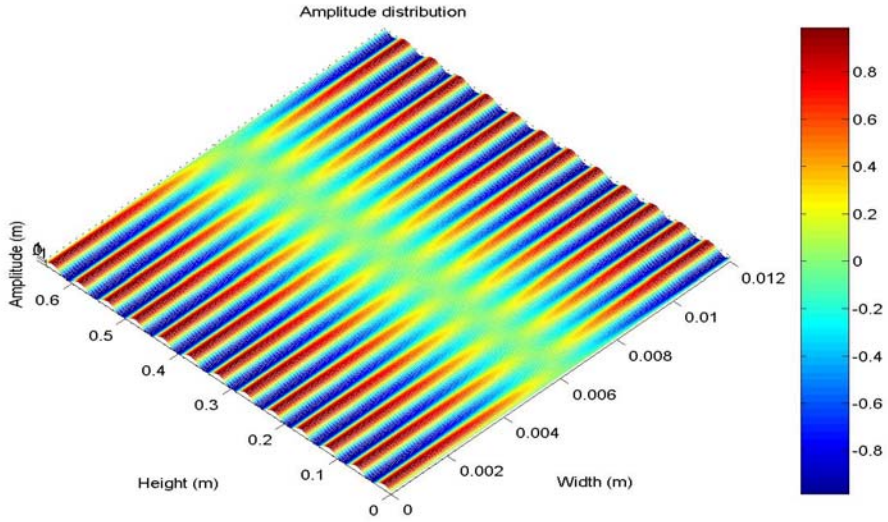

Figure 8.14 Mode 1_25 (5993.3 Hz).

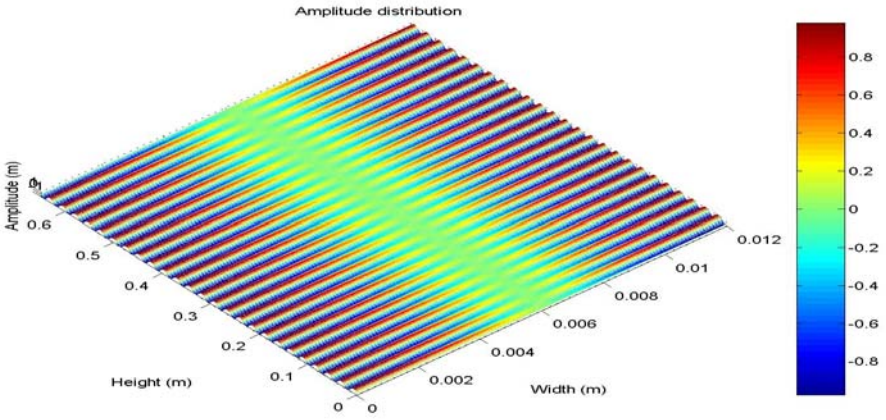

Figure 8.15 Mode 1_50 (7405.6 Hz).

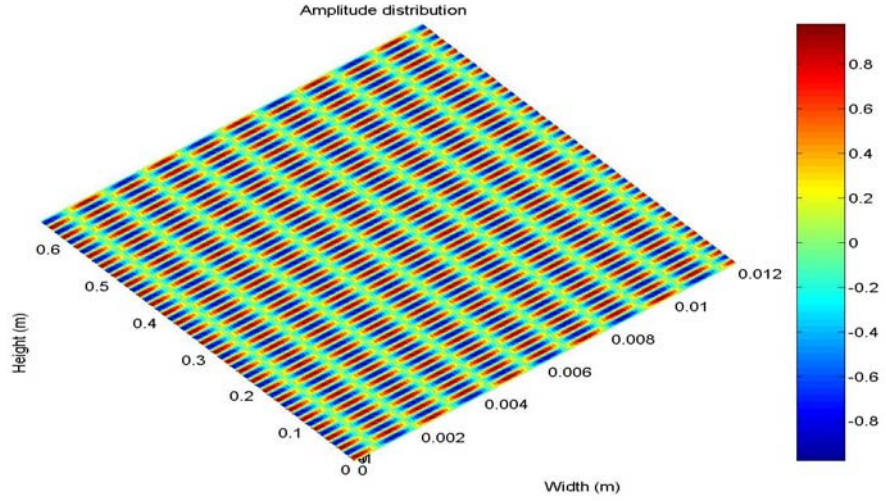

Figure 8.16 Mode 10_50 (54648 Hz).

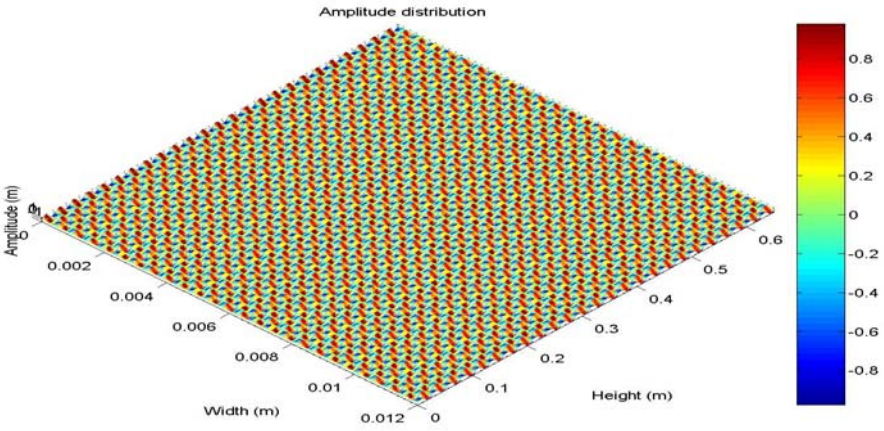

Figure 8.17 Mode 50_50 (272130 Hz).

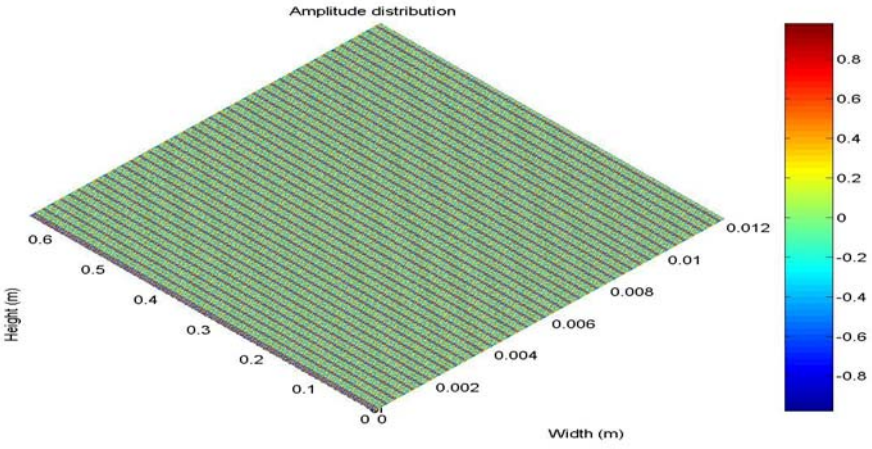

Figure 8.18 Mode 200_200 (1 GHz).

9 Conclusion and Further work

The study conducted shows that global damage detection and localization is possible by monitoring modal parameters. The fundamental frequency is shown the ability of detecting presence of damage, though inaccurately. In fact, it was shown that, for a defect in form of crack as well as local weakness, the fundamental frequency decreases with an increase in defect severity. In case of defect in form of hole, the fundamental frequency was shown to increase with increasing in the hole diameter.

Changes in the strain energies in the elements forming the crack tip show that the elemental magnitude of strain energy decreases as the crack is extended. The Strain energies increase with increasing modes, with a noticeable peak of the energy magnitude at the 12th mode at which the defect highly expresses itself leading to damage localization.

The mode-dependent energy dissipation around the defect was also shown to be a damage indicator, as shown by monitoring the 12^{th} mode for the current specimen and defect location.

This work is a contribution to the vibration-based technique by predicting the feasibility of damage detection on sheet-like (non rigid) materials at higher modes. Indeed, the displayed spatial of some of the modes shows that mode 10_50 (10^{th} mode in length direction combined with the 50^{th} mode in width direction) allows high probability of damage detection as well as the estimation of the detectable critical defect size. However, the results obtained at modes 50_50 (272.13 kHz) and 200_200 (1GHz) show the limit of vibration-based approach to damage detection, which appears to be in the range of acoustic microscopic investigation.

The analysis in this study has been performed for a defect located at half the specimen length. Subsequent work may show that moving the defect away from the initial position will lead to the same trend between the monitored (the most sensitive to the defect location) frequency and defect induction.

10 References

1. Doebling SW, Farrar CR, Prime MB, Shevitz DW. Damage identification and health monitoring of structural and mechanical systems from changes in their vibration characteristics: a literature review. Los Alamos National Laboratory report LA-13070-MS

2. Ajay S. chintalapudi, Husam M. Hassan, (2005), Investigation of methods to detect defects in thin layered materials. Master's Thesis BTH

3. Anderson T.L, Fracture Mechanics- Fundamentals and applications.

4. Parks, D.M., "A Stiffness Derivative finite element technique for determination of crack tip stress intensity factors." International Journal of fracture, Vol. 10, 1974, PP. 487-502

5. Hellen, T.K., "On the method of virtual crack extensions." International Journal for numerical methods in engineering, Vol. 9, 1975, pp. 187-207.

6. Shih, C.F., Moran, B., and Nakamura, T., "Energy Release Rate along a three dimensional crack front in a thermally stressed body." International Journal of fracture, Vol. 30, 1986, pp. 79-102

7. Moran, B. and Shih, C.F., "A General treatment of crack tip contour integrals." International journal of fracture, Vol. 35, 1987, pp. 295-310

8.http://www.memagazine.org/backissues/may98/features/wrong/wrong.html

9. Kaluvala Santhosh, (2005) Thin Layered Laminates-Testing and Analysis. Master's Thesis BTH.

10. ABAQUS Users Manual 6.3 (CAE and Explicit).

11. http://web.mit.edu/sskess/www/papers/SPIE01.pdf

12. Göran Broman, (2003) Computational Engineering.

Appendix A - FEM Model

A.1 Element

The element used for construction of the mesh was a four node shell membrane element. The four nodded element has the advantages of simplicity and efficiency. Hence they have been used.

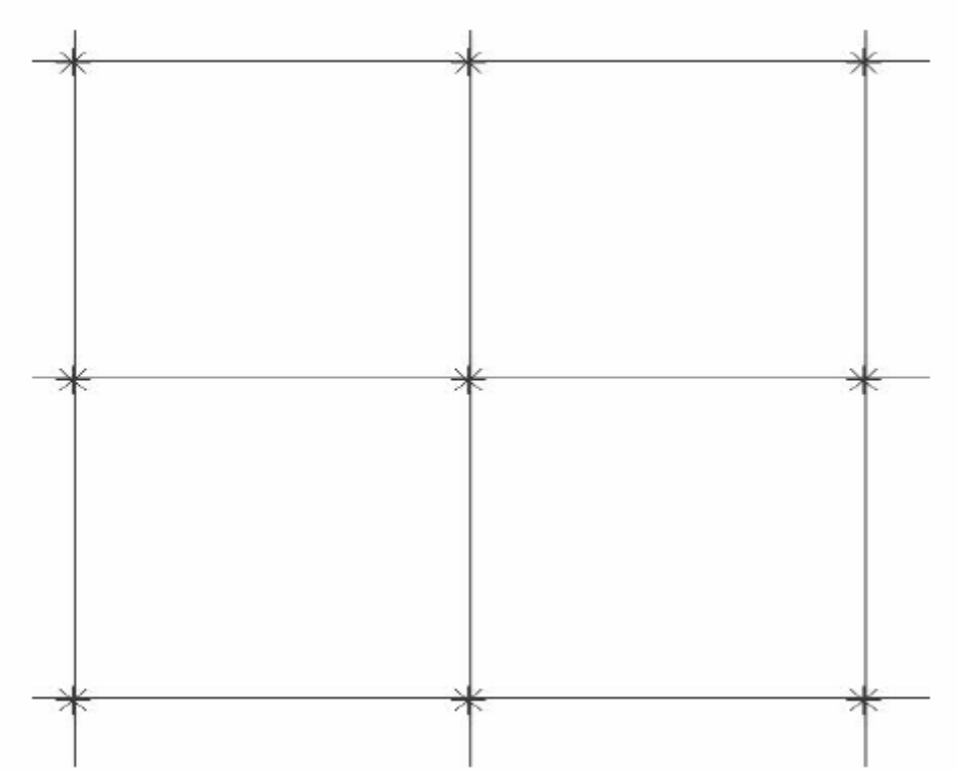

*Figure A.1 a set of four-node elements in a mesh. The * indicates the nodes while the lines are the element boundaries.*

A.2 Local weakness

The model is divided into three partitions P1, P2 and P3. The rigidity is constantly reduced in steps of 2% to the original value, introducing the local weakness. The rigidity in P2 has been subjected to constant reduction in rigidity from the original value as suggested by table A.6, A.7, A.8 and the fundamental frequencies are recorded. The rigidities in P1 and P3 were kept constant throughout the analysis. The model has been analyzed for different lengths of P2 as can be seen in A.5.

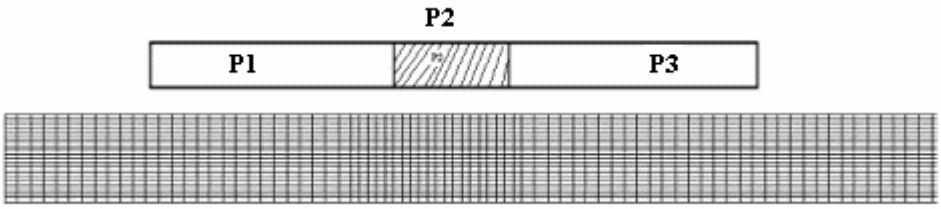

Figure A.2 FEM Model for local weakness. Refined elements can be seen at the locally weak area, while coarse mesh at the un-defected areas.

A.3 Hole

The model has been divided into three partitions P1, P2 and P3. The partition in this case has been created to have a finer mesh at the defect as can be seen below. The Mechanical and physical properties have been taken from the table 7.3.

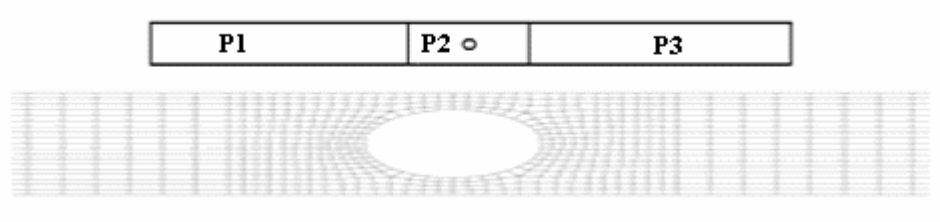

Figure A.3 FEM Model for Hole. Refined elements can be seen at near to the hole, while coarse mesh at the un-defected areas.

A.3 Crack

The model has been divided into three partitions P1, P2 and P3. The partition in this case has been created to have a finer mesh at the defect as can be seen below. The Mechanical and physical properties have been taken from the table 7.3.

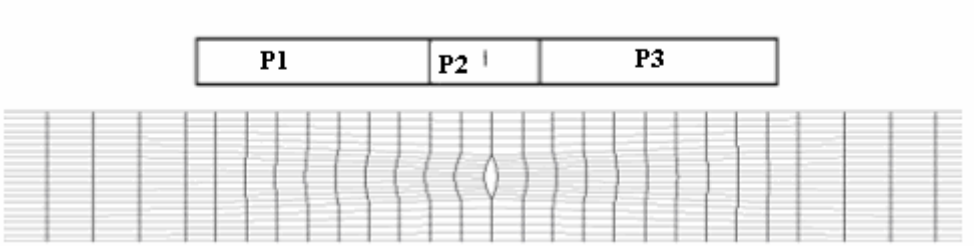

Figure A.3 FEM Model for crack. Refined elements can be seen at near to the crack, while coarse mesh at the un-defected areas.

A.4 Tables

Table A.1 Convergence Test for partition P_1 and P_3.

Element Size m^2	Fundamental Frequency Hz
0.00003	99.497
0.00006	99.497
0.00001	99.497
0.0003	99.498
0.0006	99.498
0.001	99.5
0.0015	99.502

Table A.2 Convergence Test for partition P_2.

Element Size m^2	Fundamental Frequency Hz
0.000624	99.543
0.000810	99.543
0.000882	99.544
0.000975	99.544
0.001083	99.545
0.001218	99.546
0.0015378	99.479
0.0020625	99.518

Table A.3 relation of crack length with Fundamental frequency.

Crack Length m	Fundamental Frequency Hz
0	99.544
0.004	99.551
0.0057	99.531
0.0073	99.494
0.0088	99.431

Table A.4 relation of hole diameter with Fundamental frequency.

Hole Diameter m	Fundamental Frequency Hz
0	99.544
0.0004	99.565
0.001	99.592
0.002	99.712
0.003	99.883
0.004	99.955

Table A.5 relation of locally weak area with Fundamental frequency.

Defect Area m^2	Fundamental Frequency Hz
0	99.544
3.6×10^{-5}	99.516
6×10^{-5}	99.497
7.2×10^{-5}	99.488

Table A.6 relation of frequency with locally weak area when the area is maintained constant (3.6×10^{-5}) and rigidity is reduced with constant intervals.

Young's Modulus Mpa	Percentage Reduction in Rigidity	Fundamental Frequency Hz
8e9	0	99.544
784e7	2	99.516
76832e5	4	99.488
7529536e3	6	99.459
7378945280	8	99.430

Table A.7 relation of frequency with locally weak area when the area is maintained constant (6×10^{-5}) and rigidity is reduced with constant intervals.

Young's Modulus Mpa	Percentage Reduction in Rigidity	Fundamental Frequency Hz
8e9	0	99.544
784e7	2	99.497
76832e5	4	99.451
7529536e3	6	99.403
7378945280	8	99.355

Table A.8 relation of frequency with locally weak area when the area is maintained constant (7.2×10^{-5}) and rigidity is reduced with constant intervals.

Young's Modulus Mpa	Percentage Reduction in Rigidity	Fundamental Frequency Hz
8e9	0	99.544
784e7	2	99.488
76832e5	4	99.432
7529536e3	6	99.376
7378945280	8	99.318

A.5 Steps in construction

1. Part Module: A geometry based part is created, using the ‘partition’ tool box the part was divided into three sub-parts. This partition is used to allot different meshing resolutions for the defected regions and also to assign different Young’s modulus for the introduction of local weakness. For the control specimen no such partition was created.

2. Property Module: A material is created followed by the creation of the section and then assigning the material and the section to the specimen. The mechanical and physical properties were used as given in the table 7.3 Two materials were created for the defect type of local weakness.

3. Assembly module: Assembly module is used to create instances of our parts and to position the instances relative to each other. Since we have only one structure we select the part to be independent in the assembly module environment.

4. Step Module: Step module is used to create analysis steps, specify output requests etc. A step is created and static general type analysis is selected. The required output Eigen frequencies and strain energies is requested here.

5. Boundary condition Module: Boundary condition representing the clamping without any degree of freedom in any direction is created using the ‘encastre’ option is selected. The specimen is clamped at both the ends.

6. Mesh Module: The element type ‘M3D4R’ is selected followed by the seeding of the specimen along the edges. The elements are then generated along the seeds.

7. Job Module: We create and submit the job here.

8. Visualization module: The results can be visualized here. The results can also be obtained in various forms like the .odb file, .dat file.

The above steps relate to the control specimen and the idea behind damaged specimens has been described earlier.

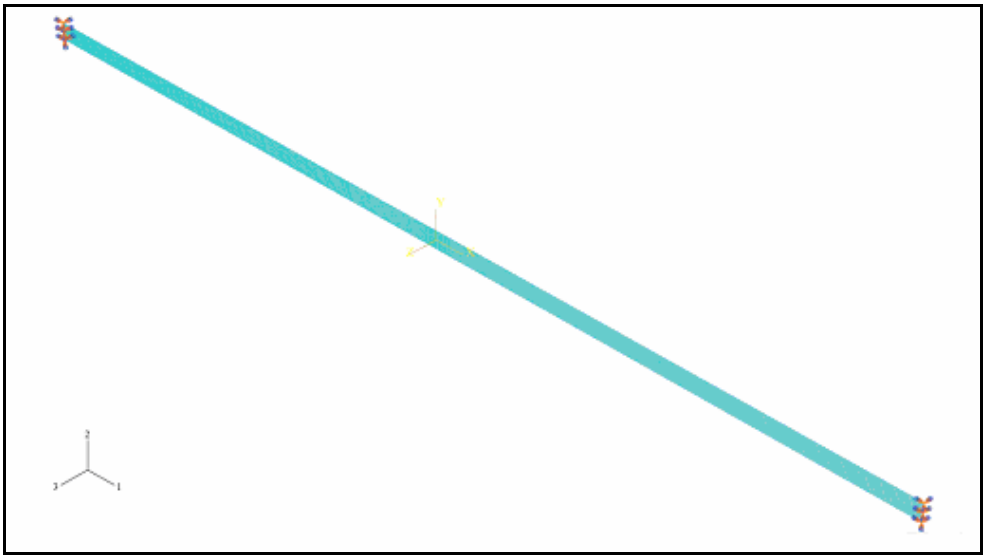

Figure A.4 showing the control specimen with the clamped boundary conditions

Appendix B - Abaqus Codes

The dots between the codes represent the deleted part due to its large size. The deleted part contains nodes and elements defining the geometry of the specimen and can be automatically generated in Abaqus CAE.

B.1 Control Specimen

```
*Heading
Control Specimen
** Job name: intact model Model name: Model-1
*Preprint, echo=NO, model=NO, history=NO, contact=NO
**
** PARTS
**
*Part, name=Part-1
*End Part
**
**
** ASSEMBLY
**
*Assembly, name=Assembly
**
*Instance, name=Part-1-1, part=Part-1
*Node
      1, -0.00999999978, -0.00600000005,          0.
      2, -0.00999999978,  0.00600000005,          0.
      3, -0.324999988,    0.00600000005,          0.
                        .
                      .
                      .

*Element, type=M3D4R
1,    1,    9,  959,  464
2,    9,   10,  960,  959
3,   10,   11,  961,  960
4,   11,   12,  962,  961
*Nset, nset=_PickedSet3, internal, generate
```

```
   1,  9261,     1
*Elset, elset=_PickedSet3, internal, generate
   1,  8800,     1
** Region: (Section-1:Picked)
*Elset, elset=_PickedSet3, internal, generate
   1,  8800,     1
** Section: Section-1
*Membrane Section, elset=_PickedSet3, material=Material-1
0.0001,
*End Instance
**
*Nset, nset=_PickedSet4, internal, instance=Part-1-1
   3,   4, 237, 238, 239, 240, 241, 242, 243, 244, 245, 246, 247, 248, 249,
250
 251, 252, 253, 254, 255
*Elset, elset=_PickedSet4, internal, instance=Part-1-1, generate
 4181,  4200,     1
*Nset, nset=_PickedSet5, internal, instance=Part-1-1
   7,   8, 731, 732, 733, 734, 735, 736, 737, 738, 739, 740, 741, 742, 743,
744
 745, 746, 747, 748, 749
*Elset, elset=_PickedSet5, internal, instance=Part-1-1, generate
 8781,  8800,     1
*End Assembly
**
** MATERIALS
**
*Material, name=Material-1
*Density
684.,
*Elastic
 8e+09, 0.38
** ----------------------------------------------------------------
**
** STEP: Step-1
**
*Step, name=Step-1
Step_Eigen
*Static
1., 1., 1e-05, 1.
```

```
**
** BOUNDARY CONDITIONS
**
** Name: BC-1 Type: Symmetry/Antisymmetry/Encastre
*Boundary
_PickedSet4, ENCASTRE
** Name: BC-2 Type: Symmetry/Antisymmetry/Encastre
*Boundary
_PickedSet5, ENCASTRE
**
** OUTPUT REQUESTS
**
*Restart, write, frequency=0
**
** FIELD OUTPUT: F-Output-1
**
*Output, field
*Element Output, directions=YES
ELEDEN, ELEN, ENER
**
** HISTORY OUTPUT: H-Output-1
**
*Output, history, variable=PRESELECT
*End Step
*Step
 Step-1: Frequency Analysis
*Frequency,eigensolver=lanczos
 15,1.,10000.,1.
**Nset,Nset=DODO
**370,371,372
**Node file,nset=DODO,frequency=1
 **U,PU
*ELPRINT
 ELSE
**
*End step
```

B.2 Model with a crack

```
*Heading
 dfd
** Job name: cr_4 Model name: Model-1
*Preprint, echo=NO, model=NO, history=NO, contact=NO
**
** PARTS
**
*Part, name=Part-1
*End Part
**
**
** ASSEMBLY
**
*Assembly, name=Assembly
**
*Instance, name=Part-1-1, part=Part-1
*Node
      1, 0.00999999978,  0.00600000005,          0.
      2, 0.00999999978, -0.00600000005,          0.
      3,  0.324999988, -0.00600000005,           0.
      4,  0.324999988,  0.00600000005,           0.
                                          .
                                          .
                                          .

*Element, type=M3D4R
   1,    1,   11,  979,  466
   2,   11,   12,  980,  979
   3,   12,   13,  981,  980
   4,   13,   14,  982,  981

                                          .
                                          .


*Element, type=M3D3
8789,   10, 9049, 9058
```

```
8790,   10, 9109, 9108
8791,   10, 9058, 9067
8792,   10, 9110, 9109
                                        .
                                        .
*Nset, nset=_PickedSet3, internal, generate
   1,  9264,     1
*Elset, elset=_PickedSet3, internal, generate
   1,  8800,     1
** Region: (Section-1:Picked)
*Elset, elset=_PickedSet3, internal, generate
   1,  8800,     1
** Section: Section-1
*Membrane Section, elset=_PickedSet3, material=Material-1
0.0001,
*End Instance
**
*Nset, nset=_PickedSet4, internal, instance=Part-1-1
   7,   8, 695, 696, 697, 698, 699, 700, 701, 702, 703, 704, 705, 706, 707,
708
 709, 710, 711, 712, 713
*Elset, elset=_PickedSet4, internal, instance=Part-1-1, generate
 8381,  8400,     1
*Nset, nset=_PickedSet5, internal, instance=Part-1-1
   3,   4, 239, 240, 241, 242, 243, 244, 245, 246, 247, 248, 249, 250, 251,
252
 253, 254, 255, 256, 257
*Elset, elset=_PickedSet5, internal, instance=Part-1-1, generate
 4181,  4200,     1
*End Assembly
**
** MATERIALS
**
*Material, name=Material-1
*Density
684.,
*Elastic
 8e+09, 0.38
** ----------------------------------------------------------------
```

```
**
** STEP: Step-1
**
*Step, name=Step-1
asa
*Static
1., 1., 1e-05, 1.
**
** BOUNDARY CONDITIONS
**
** Name: BC-1 Type: Symmetry/Antisymmetry/Encastre
*Boundary
_PickedSet4, ENCASTRE
** Name: BC-2 Type: Symmetry/Antisymmetry/Encastre
*Boundary
_PickedSet5, ENCASTRE
**
** OUTPUT REQUESTS
**
*Restart, write, frequency=0
**
** FIELD OUTPUT: F-Output-1
**
*Output, field
*Element Output, directions=YES
ELEDEN, ELEN, ENER
**
** HISTORY OUTPUT: H-Output-1
**
*Output, history, variable=PRESELECT
*End Step
*Step
 Step-1: Frequency Analysis
*Frequency,eigensolver=lanczos
 15,1.,10000.,1.
**Nset,Nset=DODO
**370,371,372
**Node file,nset=DODO,frequency=1
 **U,PU
*ELPRINT
```

```
 ELSE
**
*End step
```

B.3 Model with a hole

```
*Heading
 Hole 5
** Job name: h5 Model name: Model-1
*Preprint, echo=NO, model=NO, history=NO, contact=NO
**
** PARTS
**
*Part, name=Part-1
*End Part
**
**
** ASSEMBLY
**
*Assembly, name=Assembly
**
*Instance, name=Part-1-1, part=Part-1
*Node
      1, 0.00999999978, -0.00600000005,          0.
      2,  0.324999988, -0.00600000005,          0.
      3,  0.324999988, 0.00600000005,          0.
      4, 0.00999999978, 0.00600000005,          0.

                                                .
                                                .
                                                .
*Element, type=M3D4R
   1,    1,   28, 1014,   27
   2,   28,   29, 1015, 1014
   3,   29,   30, 1016, 1015
   4,   30,   31, 1017, 1016

                                                .
```

```
*Nset, nset=_PickedSet3, internal, generate
   1,  8741,     1
*Elset, elset=_PickedSet3, internal, generate
   1,  8252,     1
** Region: (Section-1:Picked)
*Elset, elset=_PickedSet3, internal, generate
   1,  8252,     1
** Section: Section-1
*Membrane Section, elset=_PickedSet3, material=Material-1
0.0001,
*End Instance
**
*Nset, nset=_PickedSet4, internal, instance=Part-1-1
   6,   7, 690, 691, 692, 693, 694, 695, 696, 697, 698, 699, 700, 701, 702,
703
 704, 705, 706
*Elset, elset=_PickedSet4, internal, instance=Part-1-1, generate
 4200,  7770,   210
*Nset, nset=_PickedSet5, internal, instance=Part-1-1
   2,   3, 237, 238, 239, 240, 241, 242, 243, 244, 245, 246, 247, 248, 249,
250
 251, 252, 253, 254
*Elset, elset=_PickedSet5, internal, instance=Part-1-1, generate
  210,  3990,   210
*End Assembly
**
** MATERIALS
**
*Material, name=Material-1
*Density
684.,
*Elastic
 8e+09, 0.38
** ----------------------------------------------------------------
**
** STEP: Step-1
**
*Step, name=Step-1
Step_Eigen
*Static
```

```
1., 1., 1e-05, 1.
**
** BOUNDARY CONDITIONS
**
** Name: BC-1 Type: Symmetry/Antisymmetry/Encastre
*Boundary
_PickedSet4, ENCASTRE
** Name: BC-2 Type: Symmetry/Antisymmetry/Encastre
*Boundary
_PickedSet5, ENCASTRE
**
** OUTPUT REQUESTS
**
*Restart, write, frequency=0
**
** FIELD OUTPUT: F-Output-1
**
*Output, field, variable=PRESELECT
**
** HISTORY OUTPUT: H-Output-1
**
*Output, history, variable=PRESELECT
*End Step
*Step
 Step-1: Frequency Analysis
*Frequency,eigensolver=lanczos
 15,1.,10000.,1.
**Nset,Nset=DODO
**370,371,372
**Node file,nset=DODO,frequency=1
 **U,PU
*ELPRINT
 ELSE
**
*End step
```

B.4 Model with local weakness

```
*Heading
 LW12
** Job name: lw12 Model name: Model-1
*Preprint, echo=NO, model=NO, history=NO, contact=NO
**
** PARTS
**
*Part, name=Part-1
*End Part
**
**
** ASSEMBLY
**
*Assembly, name=Assembly
**
*Instance, name=Part-1-1, part=Part-1
*Node
      1, -0.0120000001, -0.00600000005,          0.
      2, -0.0120000001, 0.00600000005,           0.
      3, -0.324999988, 0.00600000005,            0.
      4, -0.324999988, -0.00600000005,           0.
                                                 .
                                                 .
                                                 .
*Element, type=M3D4R
   1,    1,    9, 1075,  504
   2,    9,   10, 1076, 1075
   3,   10,   11, 1077, 1076
   4,   11,   12, 1078, 1077
                                                 .
                                                 .



*Nset, nset=_PickedSet4, internal, instance=Part-1-1
```

```
   3,   4, 257, 258, 259, 260, 261, 262, 263, 264, 265, 266, 267, 268, 269,
270
 271, 272, 273, 274, 275
*Elset, elset=_PickedSet4, internal, instance=Part-1-1, generate
 4581,  4600,     1
*Nset, nset=_PickedSet5, internal, instance=Part-1-1
   7,   8, 827, 828, 829, 830, 831, 832, 833, 834, 835, 836, 837, 838, 839,
840
 841, 842, 843, 844, 845
*Elset, elset=_PickedSet5, internal, instance=Part-1-1, generate
 9941,  9960,     1
*End Assembly
**
** MATERIALS
**
*Material, name=Material-1
*Density
684.,
*Elastic
 8e+09, 0.38
*Material, name=Material-2
*Density
684.,
*Elastic
 7378945280, 0.38
** ----------------------------------------------------------------
**
** STEP: Step-1
**
*Step, name=Step-1
dfd
*Static
1., 1., 1e-05, 1.
**
** BOUNDARY CONDITIONS
**
** Name: BC-1 Type: Symmetry/Antisymmetry/Encastre
*Boundary
_PickedSet4, ENCASTRE
** Name: BC-2 Type: Symmetry/Antisymmetry/Encastre
```

```
*Boundary
_PickedSet5, ENCASTRE
**
** OUTPUT REQUESTS
**
*Restart, write, frequency=0
**
** FIELD OUTPUT: F-Output-1
**
*Output, field, variable=PRESELECT
**
** HISTORY OUTPUT: H-Output-1
**
*Output, history, variable=PRESELECT
*End Step
*Step
 Step-1: Frequency Analysis
*Frequency,eigensolver=lanczos
 15,1.,10000.,1.
**Nset,Nset=DODO
**370,371,372
**Node file,nset=DODO,frequency=1
 **U,PU
*ELPRINT
 ELSE
**
*End step
```

Appendix C – MATLAB Codes

C.1 Script for spatial modes

```
%%%%%%%%%%%%%%%%%%%%%%%%%%%%%%%%%%%%%%
clear all
clf

m=input('Enter the m value for the required mode : ');
n=input('Enter the n value for the required mode : ');
%L=input('Enter the length of the membrane (m): ');
%w=input('Enter the width of the membrane (m): ');
L=0.65; w=0.012;
[x,y] = meshgrid(0:.0001:w,0:.001:L);
 z = cos(pi.*m.*x./w).*sin(pi.*n.*y./L);
%[ri,ti]=meshgrid(-2:.2:2, -2:.2:2);
%int=interp2(X,Y,abs(Z),ri,ti,'bicubic'); mesh(int);

figure(1)

mesh(x,y,z); hold on
%Bicubic interpolation of the pressure distribution
AXIS([0 0.012 0 0.65 -1 1]);
xlabel('Width (m)');ylabel('Height (m)');zlabel('Amplitude (m)');
title('Amplitude distribution');

%%%%%%%%%%%%%%%%%%%%%%%%%%%%%%%%%%%%%%
```

C.2 Script for Eigen frequencies corresponding to the modes

```
%%%%%%%%%%%%%%%%%%%%%%%%%%%%%%%%%%%%%%%%

1%Vibration of a membrane
%Axes: x horizontal, width of the membrane, and y vertical, length of the
%membrane
%B.C.: x=0 and x=w are free, y=0 and y=L are immobile
clear all
clc

h=0.0001;  %thickness PPR
d=684; %kg/m3...density

w=0.012; %w=input('Width = ');
L=0.65; %L=input('Length = ');
T=14;%T=input('Load = ');
t=T/w;

%Wave velocity
C=sqrt(t/d/h)

%Modes
m=input('m = ');
n=input('n = ');

%Eigenfrequencies
om=sqrt(C*C*((pi*m/w)*(pi*m/w)+(pi*n/L)*(pi*n/L)));
f=om/2/pi


%%%%%%%%%%%%%%%%%%%%%%%%%%%%%%%%%%%%%%%%
```

C.3 Script Local Weakness Plot

```
%%%%%%%%%%%%%%%%%%%%%%%%%%%%%%%%%%%%%

clear all,
close all,
%first graph lw6
A=[0 2 4 6 8 10 12 14];
B=[99.544 99.516 99.488 99.459 99.430 99.400 99.366 99.335];
%second graph lw10
C=[0 2 4 6 8 10 12 14];
D=[99.544 99.488 99.432 99.376 99.318 99.259 99.191 99.130];
%third graph lw12
E=[0 2 4 6 8 10 12 14];
F=[99.544 99.479 99.414 99.348 99.281 99.213 99.133 99.063];
%Fourth graph
G=[0 2 4 6 8 10 12 14];
H=[99.544 99.461 99.378 99.293 99.208 99.120 99.019 98.929];
plot(A,B,'*-',C,D,'o-',E,F,'<-',G,H,'*-')
xlabel('Reduction in Rigidity %','FontSize',14);ylabel('Fundamental Frequency Hz','FontSize',14);
Legend ('Length = 6mm', 'Length = 12mm', 'Length = 14mm','Length = 18mm')
%%%%%%%%%%%%%%%%%%%%%%%%%%%%%%%%%%%%%
```

Department of Mechanical Engineering, Master's Degree Programme
Blekinge Institute of Technology, Campus Gräsvik
SE-371 79 Karlskrona, SWEDEN

Telephone: +46 455-38 55 10
Fax: +46 455-38 55 07
E-mail: ansel.berghuvud@bth.se